Structure of three-dimensional turbulent boundary layers

By P. Bradshaw[1] and O. Sendstad[1]

The changes that occur in the Reynolds-stress-producing motion when a cross-stream pressure gradient is applied to an initially two-dimensional turbulent flow are discussed. Two main examples are used; (i) a temporal simulation of a channel flow with crossflow applied by a spanwise pressure gradient for $t > 0$, and (ii) a spatial simulation of the boundary layer on an infinite swept wing, which is still in progress. Evidence examined to date suggests that the structural changes in the two cases are similar, but the mechanisms may be significantly different, even if effects peculiar to the viscous wall region are ignored. The results from (ii) are provisional, based on too short a time series for accurate statistical averages to be obtained. We treat turbulence "simulations" (solutions of the Navier-Stokes equations in three space dimensions and time) in the same way as experiments: both have limitations of accuracy but both are acceptable representations of real fluid flows.

1. Introduction

Several experiments and simulations have shown significant differences in turbulence structure between two-dimensional and three-dimensional turbulent wall flows; similar effects are likely to occur in free shear layers but there are no sufficiently detailed data. (Note: here, "2-D" and "3-D" refer to the statistical-average properties of the flow; instantaneously, turbulence is always 3-D.) There are two main types of 3-D flow, those where large gradients occur in only one direction (normal to the wall in the case of a boundary layer) and those where large gradients occur in both directions in the plane normal to the general flow direction (as in wing-body junction flows or vortex/boundary-layer interactions). Here we deal only with the former type. With the exception of the simulations of the Ekman layer (Coleman, Ferziger & Spalart 1990) and the related 3-D "scrubbing" flow (Spalart 1989), most work relates to the more-or-less sudden application of crossflow to an initially two-dimensional flow by the action of spanwise pressure gradient or spanwise motion of a wall. This is a convenient idealization of a typical wing boundary layer in which crossflow gradually increases with downstream distance, and has the conceptual advantage of giving the impulse response of the (non-linear) system. Despite the facts that turbulence is always instantaneously three-dimensional and that individual turbulent eddies do not see the mean flow as such, noticeable structural changes can be produced by differences of as little as 10 degrees between the direction of the external flow and that of the flow near the wall.

1 Stanford University

These structural changes imply that changes may be needed in the dimensionless empirical coefficients used in Reynolds-averaged prediction methods (since the coefficients are, by definition, structural parameters). The examples most frequently quoted are that the eddy viscosity for the component of shear stress in the "cross-stream" direction is smaller than that for the streamwise direction, and that even the latter is less than in two-dimensional flow. In general, it is incorrect to correlate empirical coefficients with the mean-flow direction because that depends on the velocity of the observer, but it is legitimate to regard the direction of the initial 2-D flow as "special" and examine perturbations in axes aligned with the initial flow direction. For long times after the start of crossflow, the initial flow direction ceases to be relevant and should in principle be replaced by some fading-memory integral of (say) the direction of the resultant shear stress. Judging from the smallness of the structural changes in the Ekman and "scrubbing" flows, compared to those in flows where crossflow is suddenly applied, the changes are mainly transient. The simplest explanation is that the eddy structure set up in a two-dimensional flow takes some time to adjust to a three-dimensional mean strain field, but when it has done so, structural parameters like the ratio of shear-stress magnitude to turbulent energy return to something near their "two-dimensional" values.

Here we offer preliminary comments on the mechanisms that lead to the structural changes. The data set which we aimed to analyze is the simulation of the spatially-varying boundary layer on a 35° "infinite" swept wing initiated at NASA Ames Research Center by Dr P. R. Spalart (now of Boeing Commercial Airplane Co.); unfortunately, fully converged statistics are not available at the time of writing. Therefore, we have devoted some time to the analysis of a time-dependent ("transient") simulation, the initially 2-D channel (closed duct) flow with spanwise pressure gradient applied for $t > 0$ (Moin, Shih, Driver & Mansour 1990). As will be shown below, the duct flow is not closely related to wing boundary layers with spanwise pressure gradients. However, the effects of mean shear in the crossflow plane, $\partial W/\partial y$, are likely to be broadly similar in the two cases.

2. The Channel Flow with Spanwise Pressure Gradient

The main results of the simulation are reported by Moin *et al.* (1990). The initial 2-D flow is the same as that of Kim, Moin & Moser (1987), with $u_\tau \delta/\nu = 180$. At $t = 0$, a spanwise pressure gradient ten times as large as the streamwise pressure gradient is applied to produce a positive z-component mean velocity, which in the central part of the flow (where W is unaffected by viscous or turbulent stresses) is just $-t(1/\rho)\partial p/\partial z$. Because $\partial W/\partial x = 0$, there is no quasi-inviscid skewing of initially-spanwise vorticity into the spanwise direction, as predicted by the Squire-Winter-Hawthorne (SWH) secondary flow theorem. Therefore, turbulence quantities are affected only in the internal layers near the walls, in which streamwise vorticity $\partial W/\partial y$ spreads out from the surface by viscous and turbulent diffusion. In the Gruschwitz/Johnston "triangular" plot of W against U in axes aligned with the centerline velocity, the slope in the outer layer is nominally half that in a spatially-developing flow which has skewed through the same angle in inviscid flow. (In the inviscid secondary-flow approximation, half the outer-layer slope in the triangular

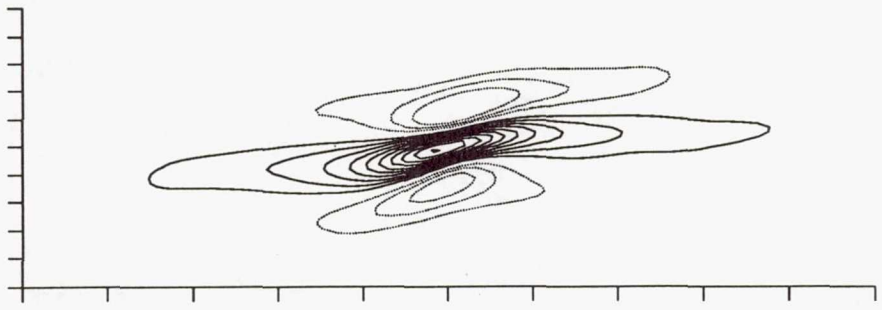

FIGURE 1. R_{12} correlation contours in channel: $x - z$ plane. In figures 1–3, negative contours are shown dotted.

plot comes from the change in coordinates from the initial x, y and half from the skewing of spanwise vortex lines to produce $\partial W/\partial y$.) After a time $t = 0.6\delta/u_\tau$, the thickness of the internal layer is about 60 wall units (one-third of the half-width of the channel), the z-component surface shear stress is about 0.68 of the original x-component surface shear stress, while the x-component surface shear stress has fallen to about 0.93 of its original value and is still decreasing; the magnitude of the surface shear stress is about 1.15 times the initial value.

The following discussion is based mainly on the two-point correlations at $t = 0.6\delta/u_\tau$ and $y^+ = 19.2$, near the peak in $-\overline{vw}$, and on budgets for various components of Reynolds stress. The correlation data are too close to the wall to be quantitatively representative of fully turbulent flow, and the bulk Reynolds number is so low that the total shear stress at $y^+ \approx 20$ in the initial flow is only 0.9 of the wall value, while the maximum in $-\rho\overline{uv}$ is less than 0.7 of the wall shear stress.

As pointed out by Moin *et al.*, the reduction in $-\overline{uv}$ seems to begin with a fall in $\overline{v\partial p/\partial y}$, which presumably implies a fall in $\overline{p\partial v/\partial y}$, the rate of transfer of turbulent kinetic energy from the u component, where it is generated, to the v component. The *last* quantity one would expect to be affected by crossflow is one that contains no z-component quantities!

Sample correlation contours in the $x - z$ and $z - y$ planes are shown in figures 1–3. At $t = 0$, the correlations are nominally symmetrical or antisymmetrical in z. At later t they are skewed in plan view and tilted in end view, by markedly differing amounts. The lengths of the axes marked on these plots are:– x, three channel half-heights or 540 wall units; y and z, one half-height or 180 wall units. For reference, the flow angle at the wall is at 36 deg. to the x axis, while at the fixed point of the correlations, $y^+ = 19.2$, the resultant mean shear and the resultant shear stress

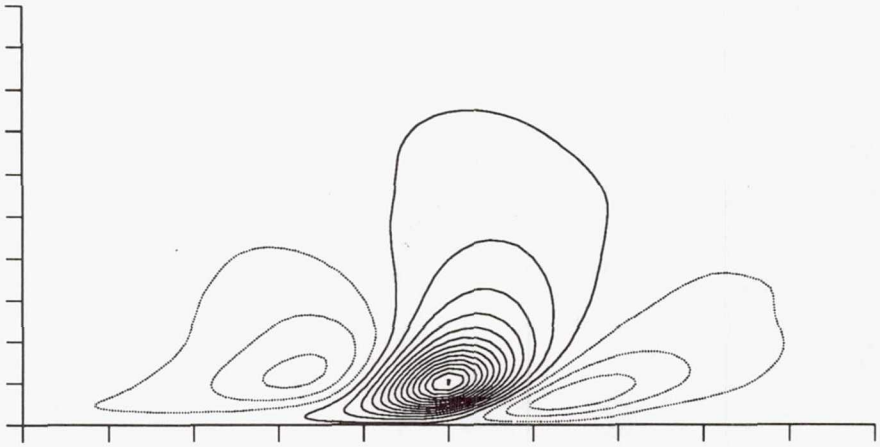

FIGURE 2. R_{11} correlation contours in channel: $z - y$ plane.

are at 13.2 deg. and 9.5 deg. to the x axis, respectively. (A large fraction of the skew in any 3-D flow occurs in the viscous wall region.) Viewed in the $x - z$ plane, the central parts of the R_{11} and R_{12} correlations (and also the R_{21} correlation, not shown here) line up with the stress angle, whereas the R_{22} correlation contours are inclined at nearly 17 deg. to the x axis and the R_{33} contours are inclined at over 20 deg. At large positive or negative separation in the x direction, the correlation contours tend to line up with the original x axis. This demonstrates quite neatly that the correlations at large separations are dominated by the unaltered eddies in the central part of the channel; this is the "inactive" motion, so called by Townsend (1961) because it is supposed to have such a small v component that it does not contribute significantly to $\overline{uv}$, and indeed the regions of R_{22} that line up with the x axis are quite small. The behavior of the negative regions that appear at large $\pm z$ in all correlations except R_{33} is interesting. In most cases, the positions of the minima are only slightly rotated away from the z axis and the contours are aligned with the central ridge, but the side extrema in R_{12} are more noticeably asymmetrical. This may give a clue to the structural alterations that reduce $\overline{uv}$.

Correlation contours in the $z - y$ plane show a wide range of behavior. R_{11} looks almost as if contours were convected passively by the w-component motion (at this time, the core fluid has moved a distance 1.8δ in the positive z direction). However, the negative side lobes have different shapes, that on the negative-z side having become slightly weaker than the other and risen above its original position ($\partial v/\partial z$ is, of course, zero, so this is not the result of passive convection). The lobe on the positive-z side seems to have been slightly flattened. The same features of shearing, upward drift of the negative-z lobe and flattening of the positive-z lobe are found in R_{12} and R_{21} (where the negative-z lobe has become slightly stronger) but are only just detectable in R_{22}.

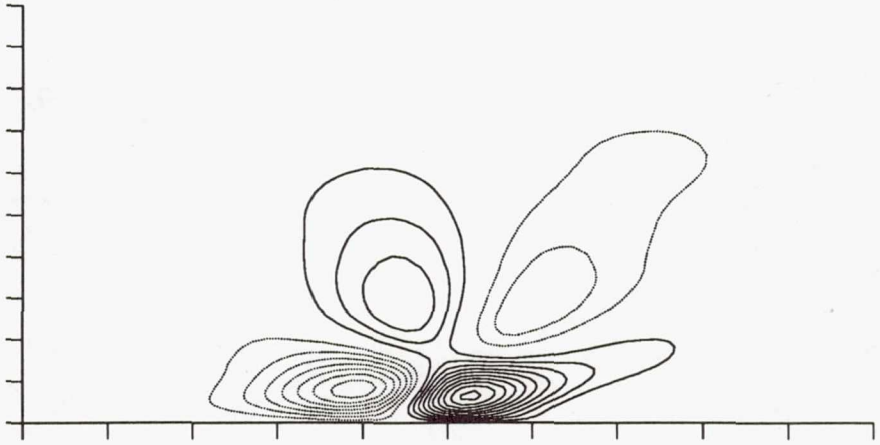

FIGURE 3. R_{13} correlation contours in channel: $z - y$ plane.

3. Simulation of the Boundary Layer on an "Infinite" Swept Wing

This simulation is intended as an approximation to the experiment of Bradshaw & Pontikos (1985) in a wind-tunnel test rig approximating a 35° "infinite" swept wing (large span and constant chord, so that mean gradients along the 35° swept generators are nominally zero).

Below, axes aligned normal and parallel to the generators are denoted by x' and z', while axes aligned with the initial flow direction ("tunnel axes") are denoted by x and z. The boundary layer initially flowed in the x direction and was then deflected in the z direction by the pressure gradient in the x' direction. This configuration is convenient experimentally because measurements need be made at only one spanwise position, and is also convenient computationally because averages can be taken along the generators as well as in time.

The numerical method and the arrangements of boundary conditions will be reported separately. Briefly, the periodic upstream and downstream boundary conditions were imposed by "fringes" in the $y - z'$ plane: the downstream fringe ingested the flow from the computational domain, removed some of its mass flow rate, and excreted the downstream. The upstream fringe was identical to the downstream one – that is, the inlet boundary layer is a greatly-thinned version of the outlet one. The run of two-dimensional flow before the onset of pressure gradient and crossflow was long enough for the perturbed boundary layer at entry to regain normal structure.

To specify the streamwise pressure gradient in the boundary layer, the normal-component velocity on the upper surface of the computational domain was chosen so that *according to an inviscid flow calculation* the pressure distribution on the lower (solid) surface was nominally the same as in the experiment. In two-dimensional flow, the representative dimensionless pressure gradient, equal to the ratio of the

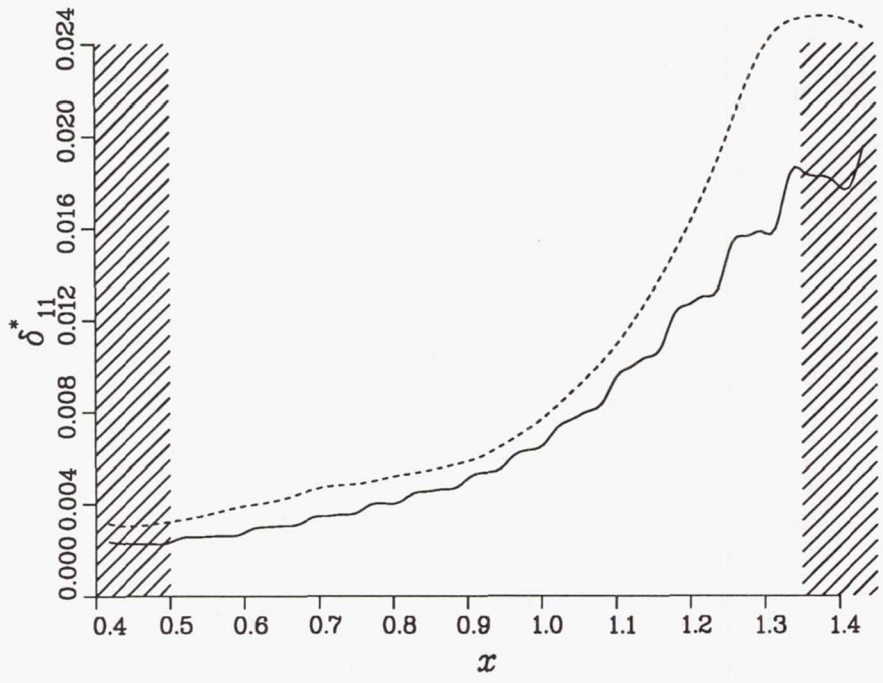

FIGURE 4. Displacement-thickness distribution in boundary layer: provisional results. Dotted line is "vorticity" definition.

two terms on the right-hand side of the momentum-integral equation

$$\frac{d(\rho_e U_e^2 \theta)}{dx} = \tau_w + \delta^* \frac{dp}{dx}, \tag{1}$$

is $(\delta^*/\tau_w)dp/dx$. Similar parameters apply in 3-D flow. The Reynolds number of the simulation is less than a tenth of that in the experiment, so typical skin-friction coefficients are larger by a factor of about two and, therefore, dp/dx must be larger by a factor of about two to reproduce the experimental distribution of $(\delta^*/\tau_w)dp/dx$.

A first estimate of the required pressure gradient gave somewhat smaller crossflow than in the experiment, but a second, larger, pressure gradient unexpectedly caused the flow to separate (i.e. the component of surface shear stress in the x' direction fell to zero). The reason was that the y-wise pressure gradient in the boundary layer is smaller than in the inviscid calculation used to determine the required normal-component velocity on the upper boundary, and as a result, the surface pressure in the retarded region is higher than in the inviscid flow; this causes increased boundary-layer growth, which further reduces $\partial p/\partial y$ and increases $\partial p/\partial x$, which causes ... and so on. The final, compromise, pressure gradient was chosen late

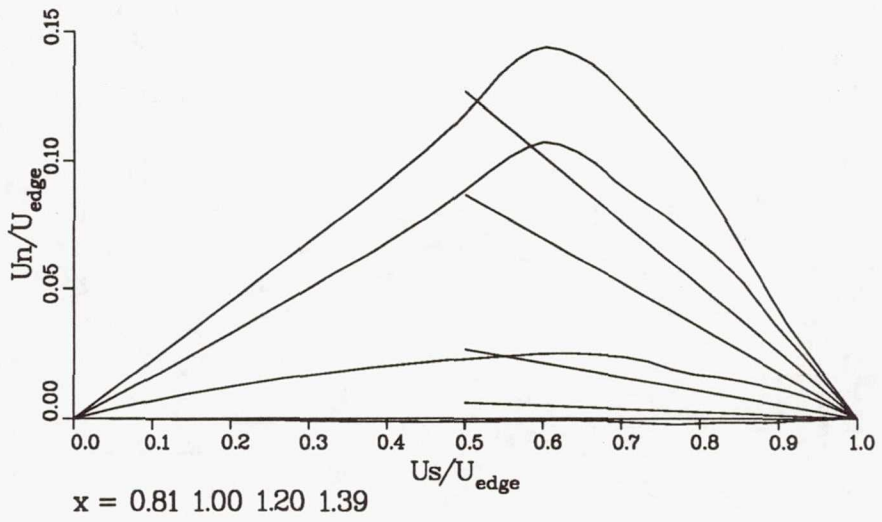

FIGURE 5. Gruschwitz/Johnston "triangular" plots in boundary layer: provisional results. x increases from lowest to highest profile.

in the summer program period, and adequately converged results for higher-order structure parameters have not been obtained at the time of writing.

Figure 4 shows the displacement thickness, which is itself not very well converged, and figure 5 the triangular plot; the adverse pressure gradient begins at about $x =$ 0.8m, where the total boundary-layer thickness is about 0.04m, and the pressure coefficient rises to just under 0.4 at the end of the useful part of the computational domain at x =1.4m.

An accompanying simulation of the 2-D boundary layer experiment of Watmuff (1990), with roughly the same distribution of $(\delta^*/\tau_w)dp/dx$, has run into unrelated numerical difficulties and is also incompletely converged. It is hoped that comparisons of the structural parameters in the 2-D and 3-D cases will allow the effects of low Reynolds number to be subtracted out, leaving an estimate of the effects of crossflow.

4. Effects of Crossflow on Turbulence Structure

Several experiments (v.d. Berg *et al.* 1975, Bradshaw & Pontikos 1985, Anderson & Eaton 1987) have shown that when a spanwise component of pressure gradient forces an initially 2-D boundary layer into crossflow, (i) the direction of the shear-stress vector $(-\overline{uv}, -\overline{vw}$ changes more slowly than the direction of the velocity-gradient vector $\partial U/\partial y, \partial W/\partial y)$ (implying that the spanwise component of eddy viscosity is smaller than the streamwise component for any reasonable definition of the arbitrary "spanwise" direction), and (ii) the ratio of shear-stress magnitude to

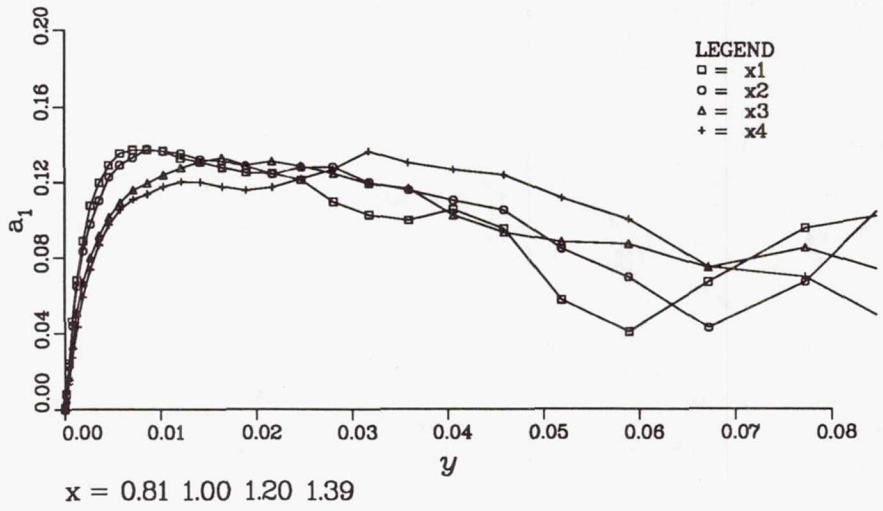

FIGURE 6. Ratio of shear stress magnitude to turbulent energy, a_1, in boundary layer: provisional results.

turbulent kinetic energy decreases (leading to a shortfall in turbulent energy production and thus to a decrease in the absolute values of turbulent energy and shear stress). Qualitatively similar results have been obtained with hot-wire anemometers and laser-doppler velocimeters, so that instrument error is not responsible. Previous low-Reynolds-number simulations of near-equilibrium flows (above) showed smaller effects, plausibly attributable to the transience of the structural changes.

The 3-D boundary-layer simulations certainly show this lag in shear-stress direction, which is qualitatively deducible directly from the Reynolds-stress transport equations (if compensating behavior of the pressure-strain redistribution term is discounted), and which is qualitatively reproduced by most transport-equation turbulence models. It is not necessarily a universal phenomenon: Johnston (1970) showed an advance, rather than a lag, in the shear-stress direction in flow over a swept step, where large values of streamline curvature, $\partial V/\partial x$, may have intervened. In the present boundary layer, $-\overline{vw}$ in the outer layer seems to be of the opposite sign to that in the inner layer; *ipso facto* this cannot be explained by turbulent transport of $-\overline{vw}$ from below.

The 3-D boundary-layer simulation which proceeded to separation showed a pronounced decrease in the ratio of shear-stress magnitude to turbulent kinetic energy, a_1, but at the time of writing, the latest statistics for the non-separating run shows no significant decrease in this structural parameter (figure 6). Roughly the same

small decrease in a_1 in the inner layer near separation occurs in the 2-D simulation, probably as the results of contributions to turbulent energy near the wall by the "inactive motion" mentioned above. Since the maximum crossflow (W/U) is almost as large in the present 3-D simulation (figure 5) as in the experiment, the absence of the decrease in stress-energy ratio cannot be explained away by hypothesizing that $a_1$is a rapidly-increasing function of crossflow.

In the experiments, the reduction in stress/energy ratio is accompanied by a reduction in the dimensionless ratio of triple products to (turbulent energy)$^{3/2}$; simulation results are not adequately converged to confirm this finding but are not in disagreement with it.

Complete budgets for all six Reynolds stresses are being accumulated. Shear-stress budgets appear to be close to equilibrium between the "generation" terms (involving mean velocity gradients) and the pressure-strain terms. This is partly misleading, because the "rapid" part of the pressure-strain term also depends on the mean velocity gradient and can be interpreted as an immediate opposition to the generation terms. If the generation terms and the "rapid" term (of opposite sign) are lumped together, their net sum is roughly equal to the "slow" part of the pressure-strain term and is not an order of magnitude larger than the mean and turbulent transport terms. Then, the shear-stress budget looks rather like the turbulent energy budget. Unfortunately, the "slow" and "rapid" parts of the pressure-strain term have not been evaluated separately in the present simulation.

5. Conclusions

Study of a previous simulation of 3-D duct flow (Moin *et al.* 1990) have shown that the distortion of the isocorrelation contours by crossflow, to first order explicable by pure convection in the crossflow shear plane, in fact involves rotation as well as shearing of the correlation pattern. In this simulation, crossflow is generated by Reynolds-stress gradients rather than by skewing of the initial spanwise vorticity, and strong crossflow is found only within the viscous wall region. Therefore, although the rotation of the correlation pattern is compatible with the idea of eddy "toppling" in crossflow advanced by Bradshaw & Pontikos (1985), it cannot be regarded as proof.

A spatially-varying boundary layer simulation is now being run in the same geometry as an (idealized) 3-D wing experiment of 10 years ago (Pontikos 1980, Bradshaw & Pontikos 1985). Again, the Reynolds number of the simulation is low enough to raise doubts about quantitative results, but the numerical accuracy of the output is not in dispute. The simulation has not yet been run long enough for statistical averages to be reliable, but when the simulation and its 2-D counterpart have run to convergence, they will provide test cases for Reynolds-averaged prediction methods and/or data for the refinement of such methods.

The 3-D boundary layer results available at the time of writing suggest that the decrease in the ratio of shear-stress magnitude to turbulent energy with increasing crossflow is not as large as has been found in several experiments; however, a previous simulation which proceeded to self-induced separation and thus incurred

significant numerical errors did show reductions of the same order as found in experiment. The present simulation suggests that the shear-stress vector in the outer layer rotates in the opposite direction to the velocity-gradient vector.

Triple products take longer to converge than second-order products; the current simulation has not run long enough for meaningful turbulent-transport terms (*derivatives* of triple products) to be extracted.

6. Acknowledgements

We are grateful to Dr. Parviz Moin for encouraging us to study the 3-D duct simulation, and to Dr. Philippe Spalart, both for planning the 3-D boundary-layer simulation and for his patient advice and guidance at all stages of this work. PB is fairly grateful to Dr. Spalart for showing that the time-lag between experiment (Pontikos 1980) and simulation is now only 10 years.

REFERENCES

ANDERSON, S. D. & EATON, J. K. 1987 Experimental study of a pressure-driven, three-dimensional, turbulent boundary layer. *AIAA J.* **25,** 1086.

V.D. BERG, B., ELSENAAR, A., LINDHOUT, J. P. F. & WESSELING, P. 1975 Measurements in an incompressible three-dimensional turbulent boundary layer, under infinite swept wing conditions, and comparisons with theory. *J. Fluid Mech.* **70,** 127.

BRADSHAW, P. & PONTIKOS, N. S. 1985 Measurements in the turbulent boundary layer on an 'infinite' swept wing. *J. Fluid Mech.* **159,** 105.

COLEMAN, G. N., FERZIGER, J. H. & SPALART, P. R. 1990 A numerical study of the turbulent Ekman layer. *J. Fluid Mech.* **213,** 313.

KIM, J., MOIN, P., & MOSER, R. 1987 Turbulence statistics in fully developed channel flow at low Reynolds number. *J. Fluid Mech.* **177,** 133.

MOIN, P., SHIH, T. H., DRIVER, D. M. & MANSOUR, N. N. 1990 Direct numerical simulation of three-dimensional turbulent boundary layer. *Phys. Fluids A.* **2** (10), 1846.

PONTIKOS, N. S. 1980 PhD thesis, Imperial College, London.

SPALART, P. R. 1989 Theoretical and numerical study of a three-dimensional turbulent boundary layer. *J. Fluid Mech.* **205,** 319.

TOWNSEND, A. A. 1961 Equilibrium layers and wall turbulence. *J. Fluid Mech.* **11,** 97.

WATMUFF, J. H. 1989 An experimental investigation of a low Reynolds number turbulent boundary layer subject to an adverse pressure gradient. *Ames/Stanford CTR Annual Research Briefs, 1988* 153.